

Investigation of the flow between a pair of circular cylinders in the flopping regime

By H. J. KIM† AND P. A. DURBIN

NASA Lewis Research Center, Cleveland, OH 44135, USA

(Received 18 September 1987 and in revised form 22 February 1988)

The wakes of a pair of circular cylinders are grossly unsteady when the cylinders are separated in a direction normal to the approaching flow by less than one cylinder diameter. The wakes flop randomly between two asymmetric states. The time-scale for the flopping is several orders of magnitude longer than the timescale of vortex shedding, and also several orders of magnitude longer than the timescale for instability of the separating shear layers. When a splitter plate is positioned suitably on the centreline of the cylinders, the flopping can be stopped and the flow made to assume either of the asymmetric states, or a symmetric steady state. For a range of plate positions a new, periodic oscillation occurs. Acoustic excitation can also destroy the flopping mean flow, replacing it by a symmetric flow.

1. Introduction

As the spacing between two circular cylinders separated in a direction normal to a uniform oncoming stream is varied, a range of flow regimes, characterized by the behaviour of the wake region, is observed. These regimes are described by Bearman & Wadcock (1973) and by Zdravkovich (1977). A regime in which the wake is grossly unsteady, apparently flip-flopping between two quasi-stable, asymmetric states occurs when the ratio of cylinder spacing, s , to cylinder diameter, d (see figure 1*c*) lies in the range 0.1 to 1.0. In the quasi-stable, asymmetric states, the flow through the gap between the cylinders is diverted toward one side or the other, and consequently the wake behind one cylinder broadens downstream, while the other wake narrows. This asymmetric wake structure is illustrated schematically by figure 1(*c*) and by the flow visualizations in Hayashi, Sakurai & Ohya (1983) and in Zdravkovich (1977). Because the wakes are not symmetric, each separating shear layer is distinct from the others: these shear layers are labelled A–D in figure 1(*c*). The flip-flopping consists of transitions from a flow with the broad wake behind one cylinder to a mirror image flow with the broad wake behind the other cylinder. This type of gross unsteadiness was first observed by Bearman & Wadcock (1973), who verified that it was a property of the flow and not of their apparatus, but who did not investigate the phenomenon in depth. Indeed, the present appears to be the first detailed look at the flopping regime.

Our experiments are divided into three parts. In the first we consider the natural flow. It is found that transitions between the two asymmetric states can be described as a Poisson stochastic process. Thus, the transitions are entirely random and have no natural period. The mean time between transitions is on the order of 10^3 times

† Present address: Thermal, Fluid and Aeronautical Engineering Research Lab, Korea Advanced Institute of Science and Technology, P.O. Box 131, Cheongryang, Seoul, Korea.

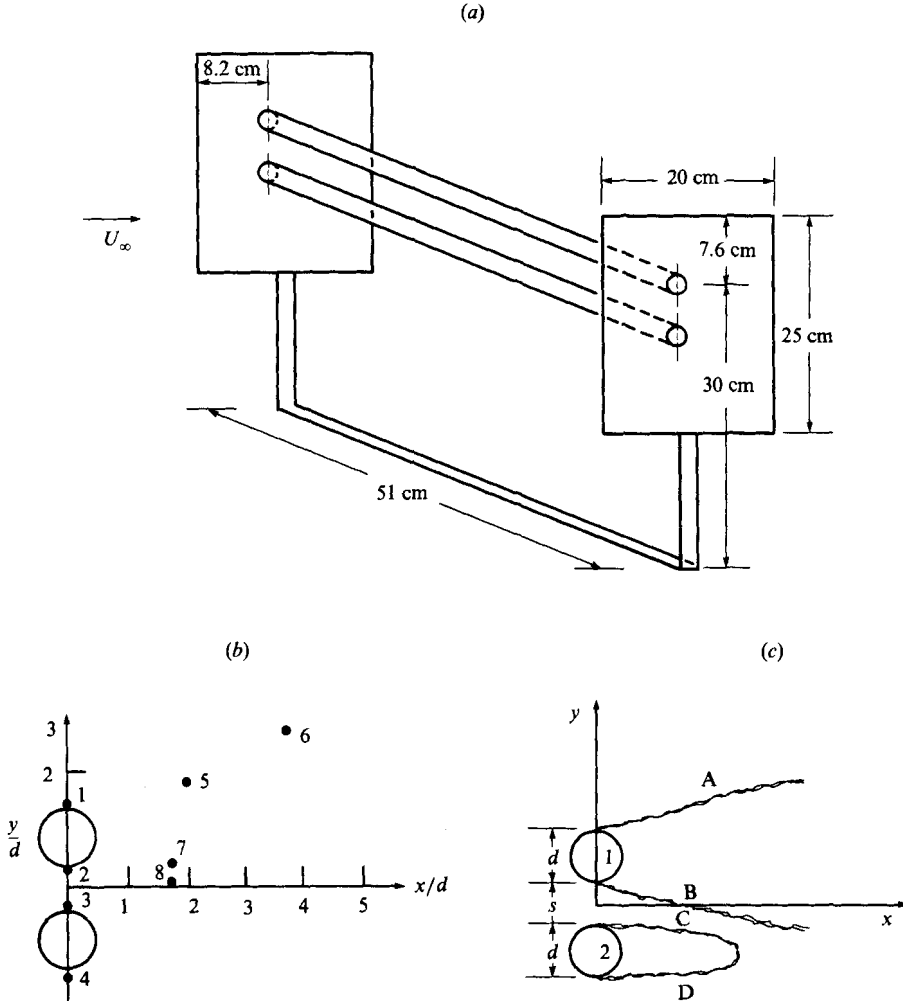


FIGURE 1. (a) Schematic of cylinder pair and free-standing endplates. The wind-tunnel blockage ratio is 7%. (b) Hot-wire measurement stations referred to in the text. (c) Schematic illustration of the asymmetric wake structure. Cylinder 1 has a broad wake, opening downstream and cylinder 2 has a narrower wake, closing downstream. The four separating shear layers are labelled A-D.

longer than the vortex-shedding period. Transitions seem to be unrelated to vortex shedding.

On a qualitative level, the unsteady flow could be considered to be a dynamic system which flips between two quasi-stable asymmetric states, which are separated by an unstable symmetric state. In the second part of our experiments, we stabilized each of these three states by placing a short splitter plate at various downstream distances along the centreline of the pair of cylinders. Hysteresis between the two asymmetric flows was observed as the plate was brought to the centreline from above or from below. For a certain range of plate positions a new periodic flow oscillation was discovered.

In the third part of our experiments, the flow was excited acoustically at the dominant shear-layer instability frequency. The period of this excitation was four orders of magnitude shorter than the mean time between flip-flops. Despite this

enormous discrepancy in timescale, the excitation destroyed the flopping and replaced it by a symmetric, steady mean flow. The excitation also decorrelated the vortex shedding on the central shear layers from that on the outer shear layers. The flow through the inter-cylinder gap appear to respond to excitation like a two-dimensional jet.

2. Apparatus

The experiments were conducted in a low-speed, open-return suction wind tunnel. The test section of this tunnel is 50 cm high, 76 cm wide, 2 m long and is preceded by a 13:1 contraction having 5 turbulence suppressing screens over its inlet. Free-stream turbulence is below 0.2%. The cylinder pair was mounted between two free-standing end plates, as illustrated by figure 1(a). The cylinder diameters, d , are 1.9 cm. The cylinder spacing, s , was adjustable by raising or lowering the bottom cylinder, but in all except the data of figures 2 and 3, s/d was kept equal to 0.75. This spacing ratio is in the flopping regime. With $s/d = 0.75$ the centreline of the cylinder pair was 3.4 cm above the centre of the test section. Because the cylinders and end plates were well away from all wind-tunnel walls, we expect the flow in the central region to be symmetric and two-dimensional in the large. Two-probe measurements were made of the spanwise coherence at the vortex-shedding frequencies. In all cases the correlation length was approximately $3d$, which is comparable with that obtained for single cylinders at similar Reynolds number (Bearman & Wadcock 1973) and shows good two-dimensionality of the flow.

Velocity measurements were made with TSI single- and cross-wire anemometers. When necessary, bridge voltages were linearized numerically after being digitized. Base pressures were measured through taps on the rear of each cylinder. These taps were connected by tubing to Setra ± 0.01 PSI pressure transducers. The frequency response of the taps plus tubing was estimated to be flat to 10 Hz.

3. The natural flow

3.1. Verification of flopping

As a spot check on our apparatus, measurements of base-pressure coefficient, C_{pb} , and vortex-shedding frequency were made at five spacing ratios. These are compared in figures 2 and 3 to data of Bearman & Wadcock (1973), shown by the solid lines. Bearman & Wadcock's data were measured at a Reynolds number of 2.5×10^4 , while ours was 3.3×10^3 . For a single cylinder, or for $s/d \rightarrow \infty$, $C_{pb} = -1.33$ at $Re = 2.5 \times 10^4$ and $C_{pb} = -1.14$ at $Re = 3.3 \times 10^3$. Therefore, quantitative discrepancies between our measurements and those of Bearman & Wadcock are to be expected.

The feature being compared in figures 2 and 3 is the existence of two distinct base pressures and vortex-shedding frequencies below $s/d = 1$, corresponding to the flopping regime, which collapse to unique values above $s/d = 1$. The double-valued region is associated with the two wakes illustrated in figure 1(c). The narrow wake has the higher shedding frequency and lower (i.e. more negative) base pressure; the wider wake has the lower shedding frequency and higher base pressure. This brief comparison is adequate to verify that our apparatus produces the flopping regime observed by Bearman & Wadcock. In order to study this regime, s/d will be set to 0.75 for the remainder of this paper.

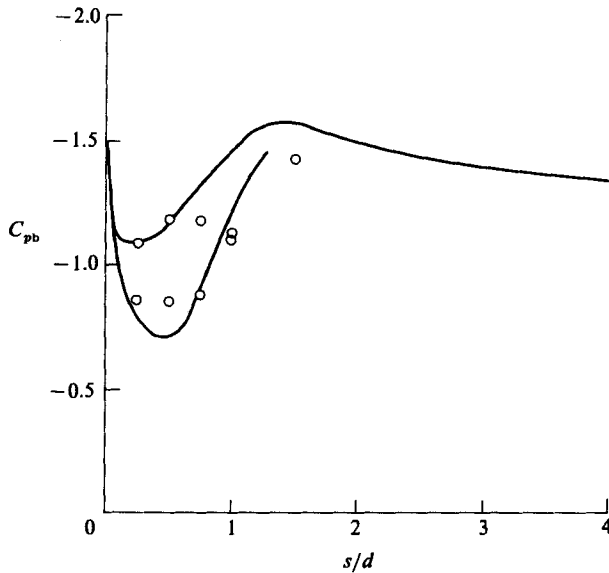


FIGURE 2. Comparison of region of bivalued pressure coefficient (circles) to measurements by Bearman & Wadcock (1973) (solid curves).

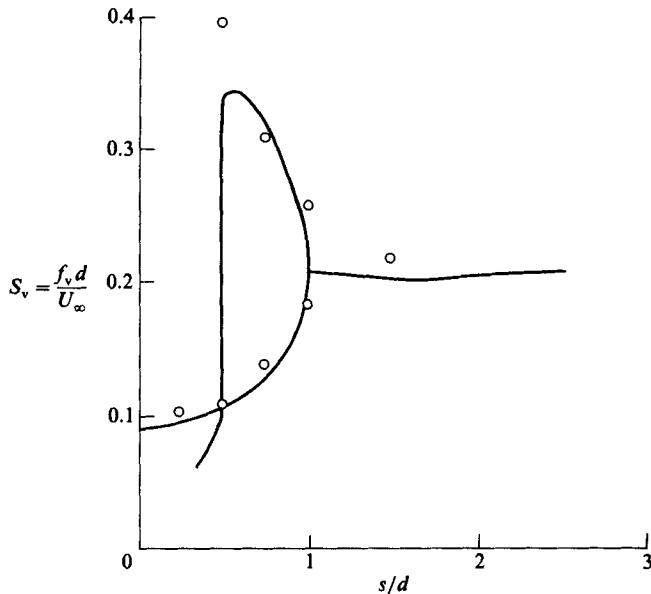


FIGURE 3. As in figure 2, but now showing vortex-shedding Strouhal numbers.

3.2. Observations of flopping

A cross-wire was positioned on the centreline, $y = 0$, of the cylinder pair at a downstream distance of $x/d = 1.6$. The flow direction was monitored simultaneously with the base pressures behind the two cylinders. Sample time histories are presented in figure 4. Flopping is manifested by the sudden changes in mean level of these curves. At this Reynolds number the transitions in flow direction and base pressure are quite sharp and it is obvious why the flow might be described as bistable. A transition from high to low C_{pb} on one cylinder is accompanied by the reverse

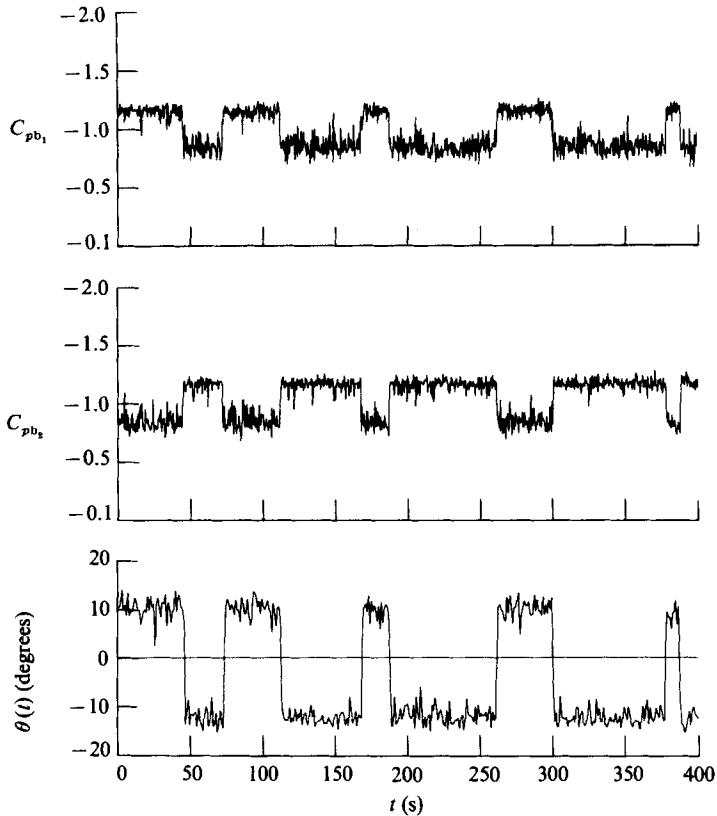


FIGURE 4. Simultaneous time histories of base pressure behind the two cylinders and of flow direction on the centreline, 1.6 diameters downstream. $Re = 3.5 \times 10^3$.

transition on the other cylinder and by a change in flow angle. The flow is always directed toward the cylinder having lower (more negative) C_{pb} : this correspondence between flow direction and C_{pb} is consistent with the lower C_{pb} being on the cylinder with the narrower wake (cylinder 2 in figure 1c). The angle measurements show less high-frequency noise simply because these data were sampled at a lower rate. The time intervals between transitions are on the order of one minute, which is three orders of magnitude longer than the vortex-shedding period. The two asymmetric flow configurations, once established, can therefore be considered quasi-steady.

The length of time between transitions appears to be random. In figure 5 we have constructed a histogram showing the probability that the interval between flips is greater than t/T , where T is the mean interval between flips. The solid line is the curve $P(t/T) = e^{-t/T}$. The histogram follows the exponential curve quite closely. A scatter plot of successive pairs of time intervals showed no evidence of correlation between transitions. This, combined with the exponential probability function, leads to the conclusion that the transitions constitute a Poisson stochastic process (Mood, Graybill & Boes, 1974, p. 122).

The variation with Reynolds number of the non-dimensional mean time interval between flips is shown in figure 6. The intervals were separated into those during which the base pressure was high on cylinder 1 (squares) and those during which it was low (circles). With the exception of the data at $Re = 3.6 \times 10^3$, the two intervals are equal within statistical error, indicating no bias in the direction of flopping. Error

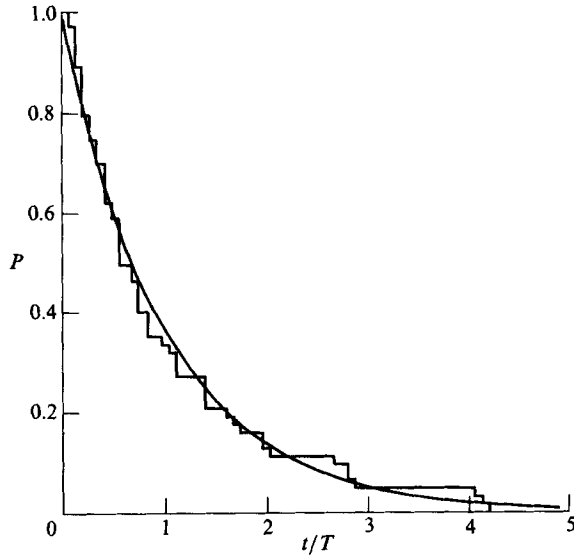


FIGURE 5. Histogram of time intervals between flips compared to an exponential curve.
 $Re = 4.1 \times 10^3$.

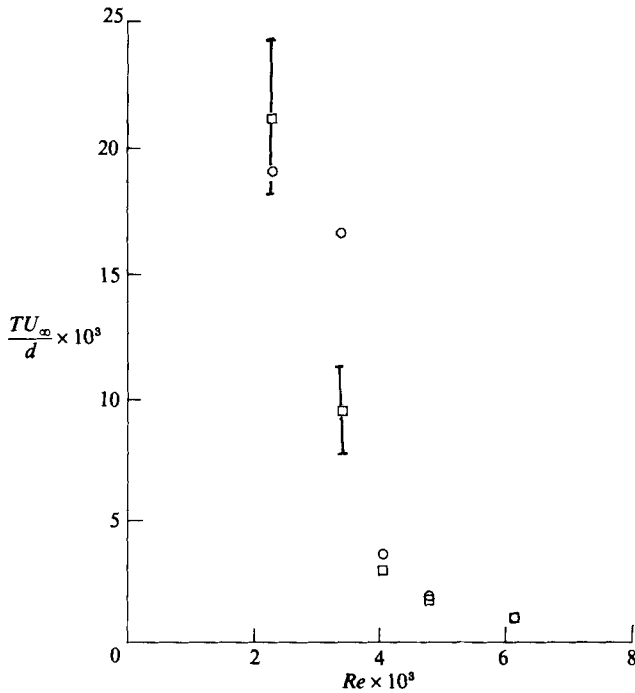


FIGURE 6. Non-dimensional mean time between flips versus Reynolds number. Circles are time intervals during which C_{pb} is low; squares are time intervals during which it is high. Error bars showing one standard deviation are included for the two lowest Reynolds numbers.

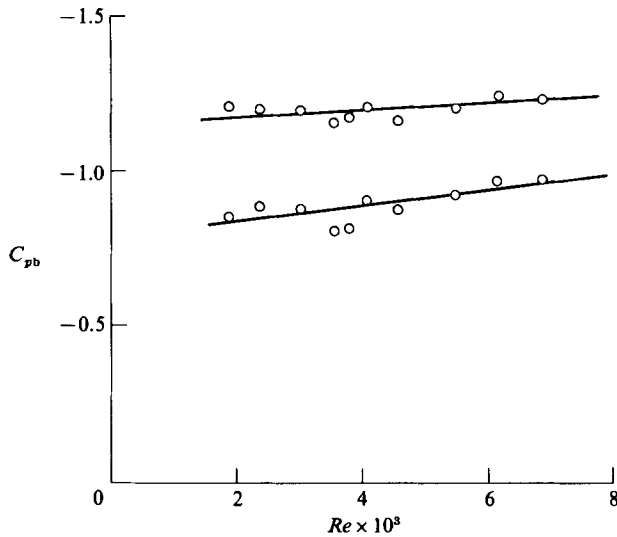


FIGURE 7. Variation with Reynolds number of the high and low levels of base pressure.

bars showing one standard deviation are included for the two lowest Reynolds numbers: the error bounds are large because the number of samples was small, owing to the long timescales involved. No reason for the discrepancy at $Re = 3.6 \times 10^3$ suggests itself, although several hours of data were required to construct these averages, and after the first half of that period the averages were within 10% of each other.

The nearly exponential decrease of $U_\infty T/d$ with increasing Reynolds number is quite surprising, as vortex-shedding Strouhal numbers are relatively independent of Reynolds number in this range. Clearly, there is no correlation between vortex shedding and flopping. At $Re = 200$ Williamson (1985) observed a steady mean flow, with no flip-flopping. If our figure 6 were extrapolated to this low Reynolds number, it would give an extremely large timescale for flopping. Thus our data are consistent with Williamson's observation.

Although the time interval between transitions is random, the magnitude of the jump in mean base pressure is essentially constant. Figure 7 shows the two levels of C_{pb} , as functions of Reynolds number. The gradual decrease of C_{pb} with increasing Reynolds number is similar to that observed behind single cylinders.

Vortex-shedding Strouhal numbers were determined from spectra measured outside the wake at position 5 in figure 1(b). Conditionally sampled spectra are presented in figure 8: the spectrum shown by a solid line was measured during time periods when cylinder 1 had a low base pressure and the spectrum shown by a dashed line was obtained during times of high pressure. It is clear that, near to the cylinders, each wake has its own distinct shedding frequency. The Strouhal numbers of the vortex-shedding peaks are plotted versus Reynolds number in figure 9. The ratio of shedding frequencies is close to, but less than, 3. Based on his low-Reynolds-number flow visualizations, Williamson (1985) suggested that the ratio of shedding frequencies might nearly be integral. Our data do not support this.

Although the narrow and wide wakes each have their own characteristic Strouhal number, the convection velocity of the shed vortices is the same in both cases. Measurements of the time delay to the peak two-point correlation as a function of probe separation were made in each of the four shear layers labelled A-D in figure

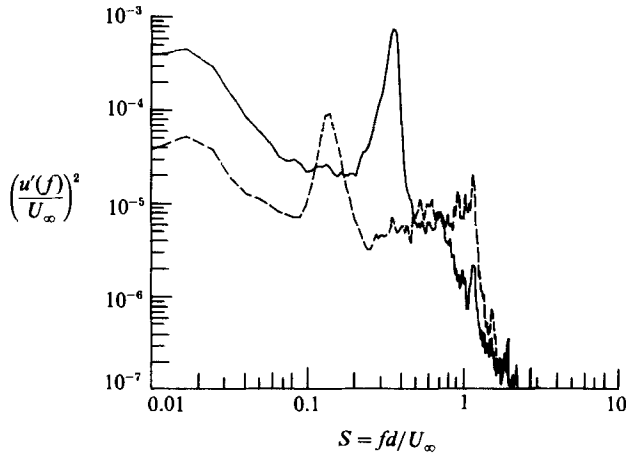


FIGURE 8. Conditional velocity spectra at station 5 during times of low (solid line) and high (dashed) base pressure on cylinder 1.

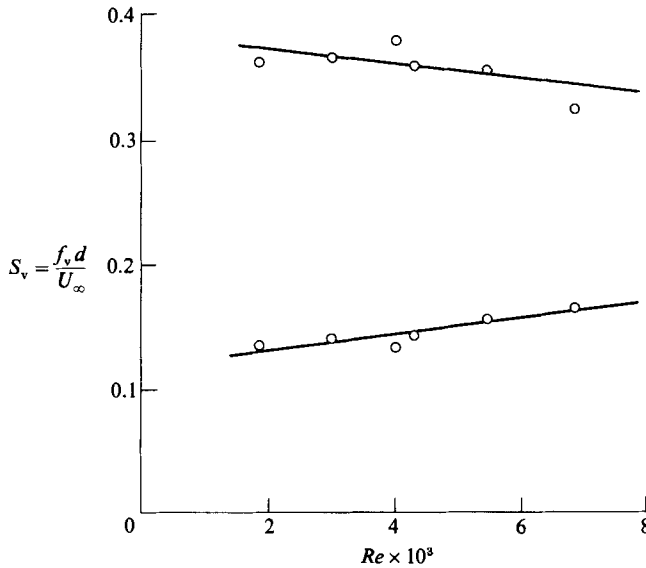


FIGURE 9. Variation with Reynolds number of the high and low values of vortex-shedding Strouhal number.

1(c). In all cases, the slope of these data gave a convection velocity of $0.8U_\infty$. The velocity along the centreline of the gap between cylinders is approximately 25% higher than U_∞ , so the convection velocity is 0.65 times the velocity on the axis of the jet emerging between the cylinders. This convection speed is typical of jet flows (Foss & Korschelt 1983).

4. The effect of a splitter plate

A short splitter plate was inserted along the centreline of the cylinders with the idea of stabilizing the two asymmetric flows and the symmetric flow: geometrical symmetry suggests that the latter exists, but apparently it is not observed because it is unstable. The splitter plate was 4.3 cylinder diameters long. The response of the

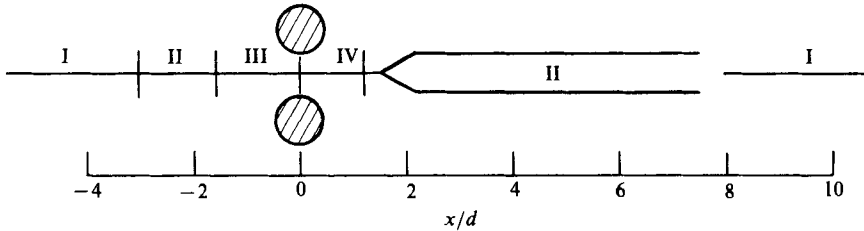


FIGURE 10. Positions of the splitter-plate leading edge for the various flow regimes observed. The band around region II shows the area where hysteresis was observed. $Re = 3.6 \times 10^3$. Roman numerals represent: I, natural flow with flopping; II, steady asymmetric flow; III, steady symmetric flow; IV, periodic oscillating flow.

flow depended significantly on the position of the plate. Figure 10 summarizes the regions in which four types of behaviour were observed. The figure shows the positions of the plate leading edge in each region. To understand the influence of the plate it must be realized that these are *leading-edge* positions and that the trailing edge is 4.3 diameters downstream. For example, the left-most region labelled I begins where the leading edge is three cylinder diameters upstream of the cylinder centres; the corresponding trailing-edge position is 1.3 diameters *downstream* of the cylinders and so protrudes into the wake area. The types of flow in the regions denoted by Roman numerals are:

- I natural flow with flopping;
- II steady asymmetric flow;
- III steady symmetric flow;
- IV periodic oscillating flow.

Region I is where the plate simply is too far upstream, or downstream to have any effect on the natural flopping.

In the region II lying between 1.2 and 7 diameters downstream of the cylinders, the flow was steady and asymmetric. The asymmetric states are illustrated by figure 1(c) and its mirror image in the x -axis. Either of the two asymmetric states could be obtained, depending on whether the plate was raised or lowered to the centreline. In fact, as the plate was raised or lowered *through* the centreline, hysteresis between the two states was observed. This hysteresis loop is shown in figure 11. In the figure, the base pressure behind cylinder 1 is shown versus the y -position of the plate. The arrows indicate the direction in which the plate was moved. The band around region II in figure 10 shows the area in which hysteresis was observed. The occurrence of hysteresis contributes to the qualitative picture of flopping being a feature of a bistable dynamical system.

The downstream region II starts where hot-wire measurements (not included in this paper) show that the turbulence intensity on the centreline begins to rise. This suggests a role of wake merging in the flopping mechanism. When the plate is inserted, it interferes with this flopping mechanism. One might suppose that as the shorter wake closes, it draws the inner shear layer (B) of the other cylinder across the centreline and opens the other wake. When it is in region II, the plate is able to prevent the layer which has been drawn across the centreline from subsequently being detrained.

Steady asymmetric flow is also established with the plate leading edge in the other region labelled II, between 1.6 and 3 diameters upstream of the cylinders. (Note that the trailing edge of the plate is still downstream of the cylinders.) It appears that an

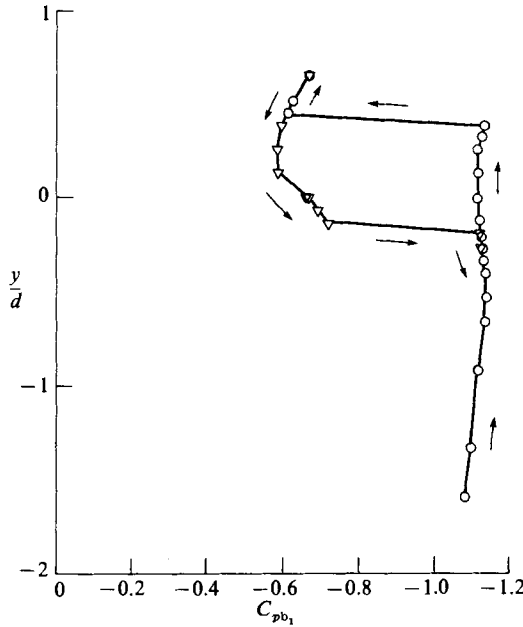


FIGURE 11. The hysteresis loop in region II.

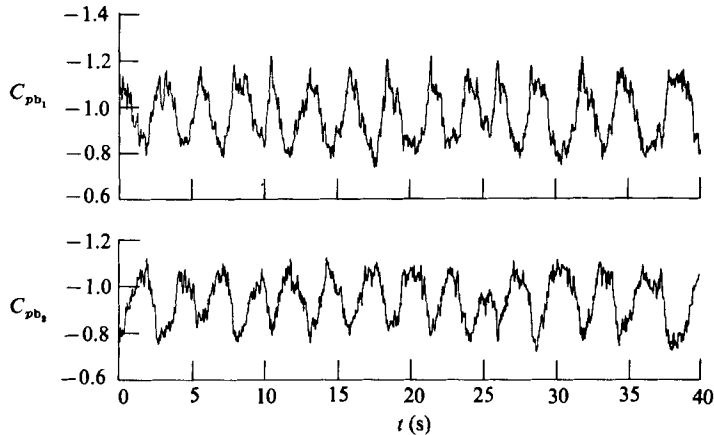


FIGURE 12. Time histories of the flow oscillation observed in region IV.

unconstrained interaction between the upstream and downstream regions II must be allowed in order for the flow to flop.

When the plate was moved to region III the flow became steady and symmetrical. Apparently, in this position the plate blocks the asymmetrical downstream development of the wakes. It would appear that when the plate is absent, the more rapid closure of the shorter wake produces a cross-stream pressure gradient which diverts the gap flow. With the plate in region III, flow toward the centreline would stagnate on the plate, producing a pressure gradient opposing wake asymmetry. In this region the mean base-pressure coefficients were the same and equal to -1.0 , which is nearly the value for a single cylinder (-1.14).

When the plate was moved further downstream to region IV, the flow went into a quasi-periodic oscillation, as shown by figure 12. The non-dimensional period of the

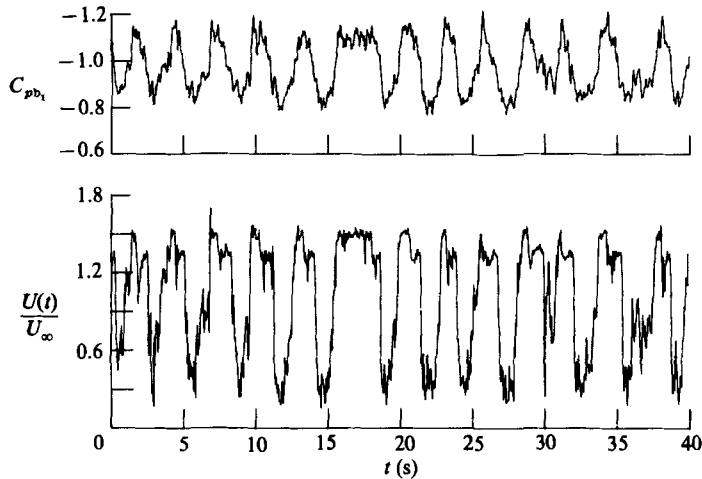


FIGURE 13. Simultaneous histories of base pressure and velocity at station 7.

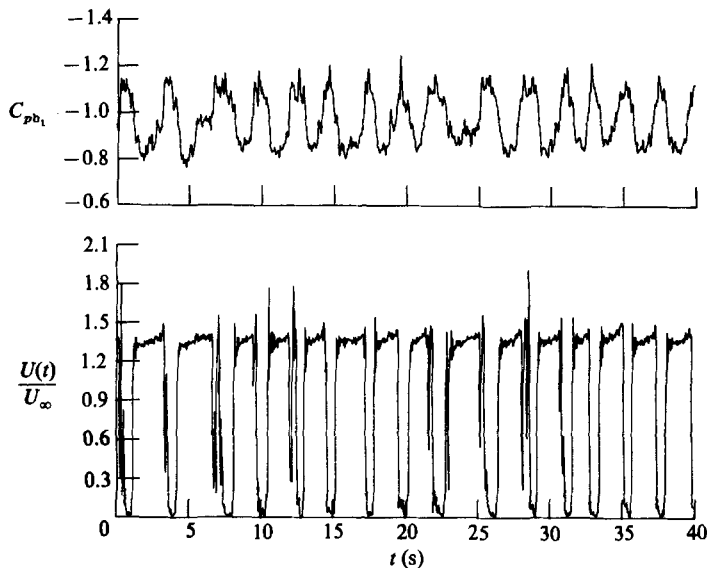


FIGURE 14. Simultaneous histories of base pressure and velocity at station 8.

oscillations was $U_{\infty} T/d = 430$ throughout region IV. For comparison to figure 6, the Reynolds number here is 3.6×10^3 . Thus, the periodic flipping is about ten times more frequent than the natural, random flipping. It is still on the order of one hundred times slower than the rate of vortex shedding.

In order to gain an insight into the cause of the flow oscillation in region IV, simultaneous measurements of the base pressure behind cylinder 1 and the flow velocity at station 7 or 8 in figure 1(b) were made. The splitter-plate leading edge was 0.7 diameters downstream, which is near the middle of region IV. Figure 13 shows a time history representative of station 7. One sees that flow accelerations occur in phase with decreases in C_{pb} ; again, this shows that the pressure drops as the wake narrows. However, when the hot wire was moved closer to the surface of the splitter plate, to station 8, a rather different behaviour was observed, as is shown by figure 14. Now the base-pressure oscillations are not in phase with the velocity. Velocity

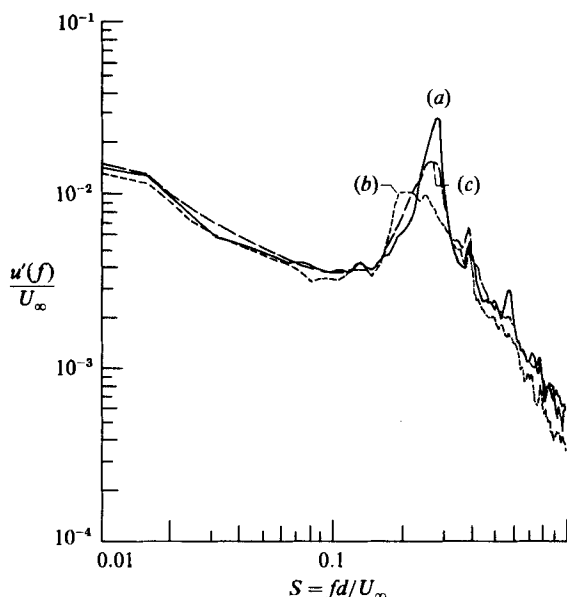


FIGURE 15. Spectra of the velocity fluctuation at station 6. Spectra (a) and (b) are conditioned on the wake behind cylinder 1 being narrow (a) or wide (b). Spectrum (c) is an unconditional spectrum.

minima occur when the base pressure is rising (because the base pressure is a negative quantity, by 'rising' we mean that it is becoming less negative); which is also when the velocity at station 7 is decelerating. As the base pressure approaches its maximum, the flow suddenly accelerates and the velocity remains high as the base pressure falls. This all suggests that the boundary layer is separating from the plate during times of rising base pressure and then reattaching when the pressure reaches its maximum: the boundary layer separates as the wake behind cylinder 1 broadens, but when that wake becomes broadest, the boundary layer suddenly reattaches. Presumably this sudden reattachment drives the flow acceleration in figure 14 and generates the periodic oscillation.

Some information on vortex shedding in the regime of periodic mean-flow oscillations is contained in figure 15. This shows measurements at station 6 (figure 1*b*) of an unconditioned spectrum, and of conditionally averaged spectra for times when cylinder 1 had a broad or a narrow wake. The broad wake still shows the lower Strouhal number, but unlike the chaotic case (figure 8), the Strouhal number is always near to 0.3.

5. The effect of acoustic excitation

Because of the marked effect that external excitation can have upon free shear layers (Wynanski & Petersen 1985), we examined its influence on the flip-flopping regime of the present parallel cylinder flow. For this purpose a loudspeaker was positioned in front of the wind-tunnel entrance and used to excite the wake flow at frequencies near the dominant shear-layer instability. The sound pressure measured in the test section was 100 dB. The dominant instability frequency in the unexcited shear layers separating from the cylinders was determined from spectra: in the range $2 \times 10^3 < Re < 8 \times 10^3$ our data were similar to those of Bloor (1964) for a single cylinder.

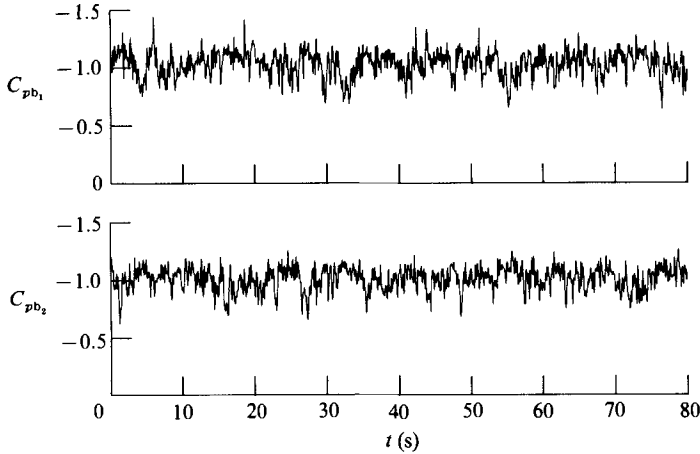


FIGURE 16. Time histories of base pressure in the presence of acoustic excitation. $Re = 3.6 \times 10^3$.

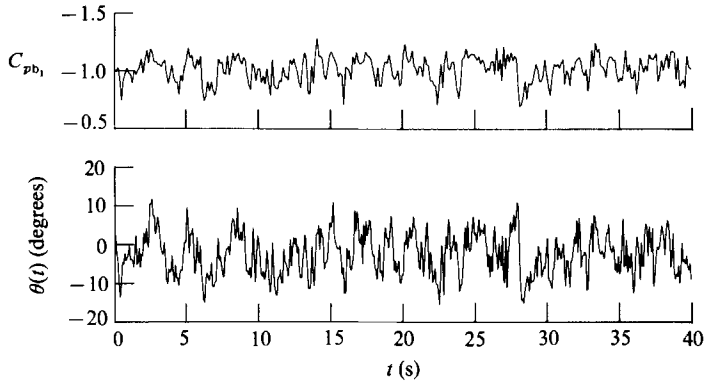


FIGURE 17. Simultaneous measurements of base pressure and centreline flow angle with excitation. Note the good correspondence of the large-scale features of these time histories.

The instability frequency was chosen for excitation because a substantial amplification of external disturbances having this frequency occurs within the shear flow. Additionally, the instability waves are ‘localized’ in the shear layers and can be generated by plane-wave excitation. Although the vortex-shedding mode is also natural to the flow, it has a symmetry, and a low frequency, which could not be produced by our loudspeaker.

Figure 16 shows that the flip-flopping is destroyed by acoustic excitation; compare figure 16 to figure 4. Excitation disrupts the flopping despite the 4 orders of magnitude discrepancy between the excitation period and the flopping timescale. In figure 16 the Reynolds number is 3.6×10^3 and excitation is at $fd/U_\infty = 1.45$. The time traces of base pressure measured with excitation (figure 16) have a tendency to mirror one another, but no clear flipping is observed. The flow direction (figure 17), measured at the same position as in figure 4, shows a high correspondence with base pressure. Thus, the larger-scale pressure variations are again associated with pulsations of the wake structure.

Cross-wire measurements were made of the two-dimensional mean flow in its natural and excited states. The profiles of velocity vectors in figure 18 are for the unexcited flow, and are conditioned on the mean base pressure behind cylinder 1.

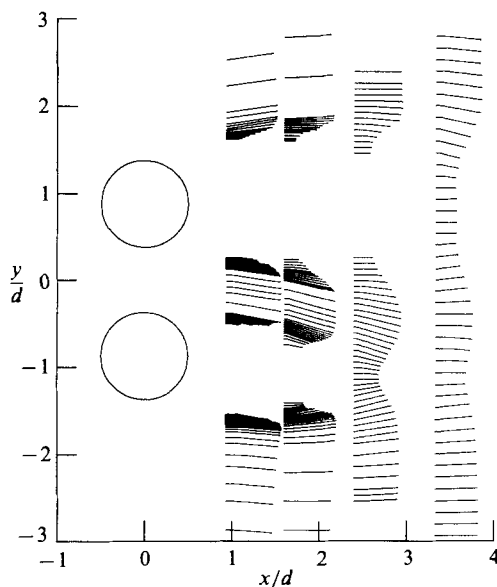


FIGURE 18. Mean velocity vectors of the wake flow during times when the base pressure behind cylinder 1 is high.

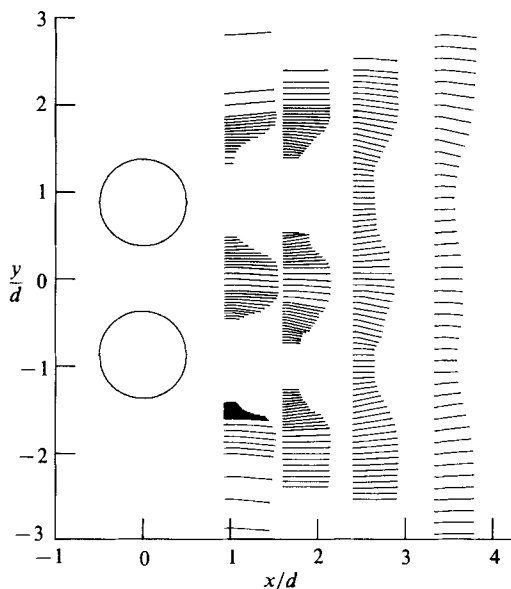


FIGURE 19. Mean velocity vectors of the wake flow with acoustic excitation.

They are measured during times when that pressure was at its higher level. The asymmetry of the wakes illustrated by figure 1(c) is shown here quantitatively, and the correspondence between the broad wake and high C_{pb} , which has been noted throughout this paper, is now substantiated. Velocities could not be measured in the near-wake region immediately behind the cylinders because flow reversal occurs there and the hot wires cannot be used. These regions are left blank in the figure.

With acoustic excitation at $fd/U_\infty = 1.45$, the mean flow field shifts to the symmetric form of figure 19. Admittedly this is unconditioned data, whereas that in

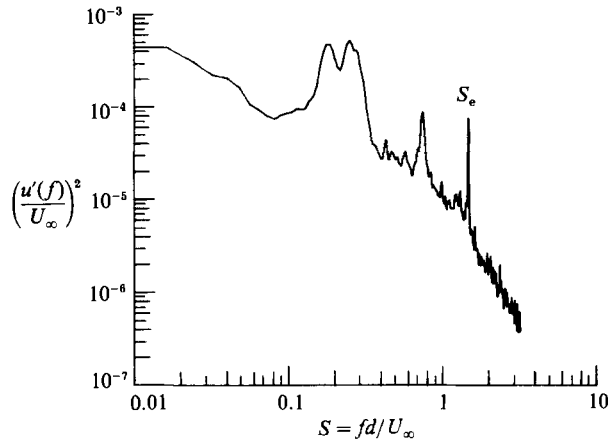


FIGURE 20. Velocity spectrum at station 5 with excitation.

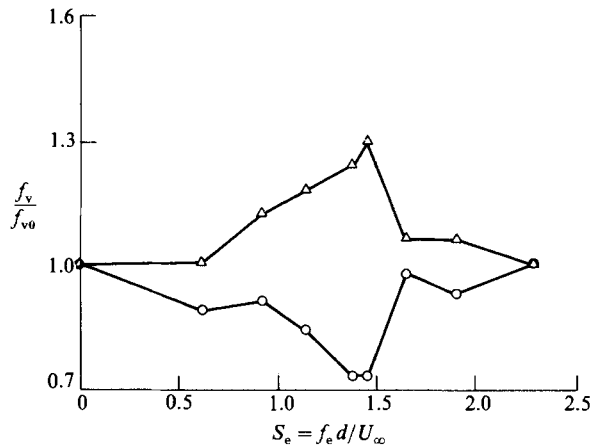


FIGURE 21. The effect of excitation frequency on vortex-shedding Strouhal numbers. Triangles are the lower frequency and circles the higher. In each case the Strouhal number is scaled on its value in the natural flow.

figure 18 is conditioned ; but the changes in flow direction under excitation (figure 17) are sufficiently rapid that this is an appropriate representation of the mean flow – in the sense that no slow, quasi-steady component can be identified.

5.1. Vortex shedding in the excited flow

Figure 20 shows a spectrum measured at station 5 (figure 1b) with excitation. Although the mean-flow flopping was stopped by the excitation, two vortex-shedding frequencies can still be discerned. The shedding frequencies have moved toward one another, but they are still distinct. One sees a peak at the subharmonic of the excitation in addition to the sharp spike at the excitation frequency itself.

Figure 21 shows the change in vortex-shedding Strouhal number caused by excitation at various frequencies. The triangles are the ratio of the lower shedding frequency to its natural value of $fd/U_\infty = 0.134$, while the circles are the ratio of the higher frequency to its natural value of $fd/U_\infty = 0.367$. The shedding frequencies experience their greatest change when excitation is at the dominant shear-layer instability frequency, $fd/U_\infty = 1.45$.

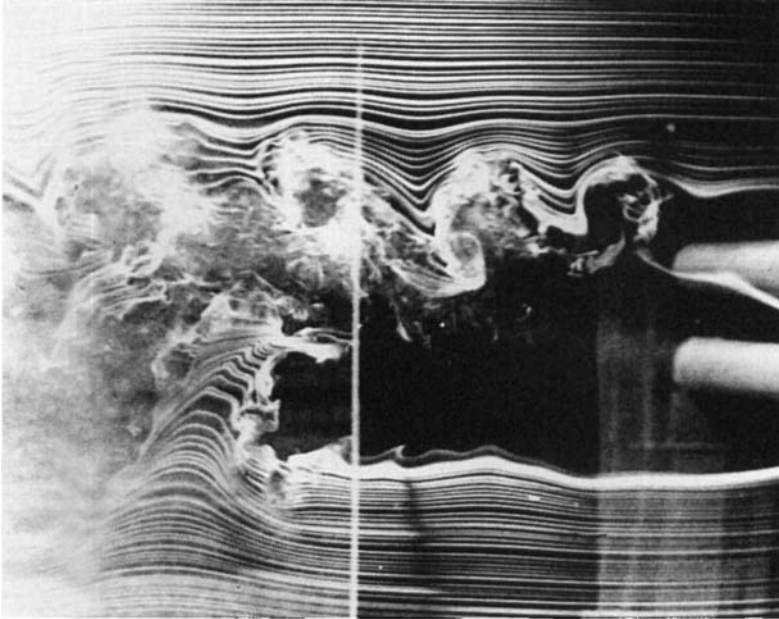
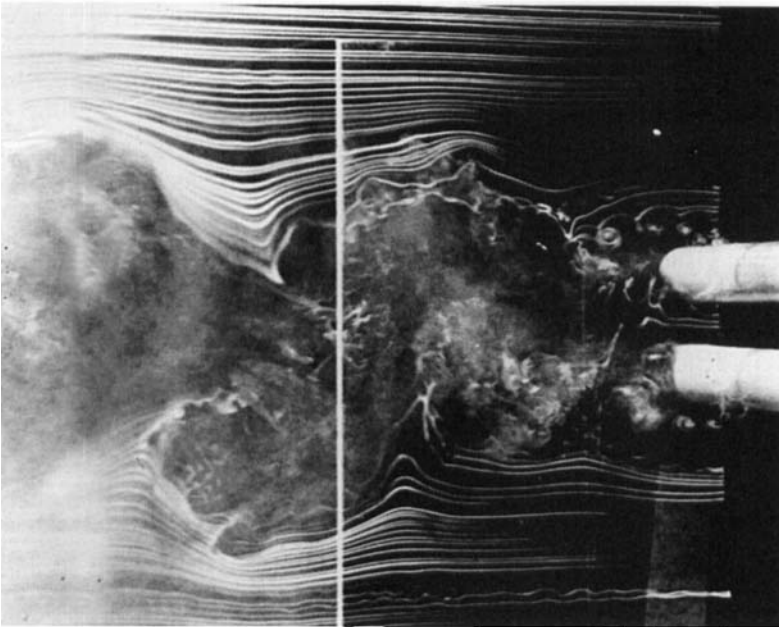
**(a) Natural****(b) Excited**

FIGURE 22. Photographs showing the natural (upper) and excited (lower) flows. The natural flow shows a highly asymmetric wake development, while the excited wake appears to be symmetric in the mean.

Further information on vortex shedding with and without excitation was obtained from unconditioned cross-spectra of coherence and phase between points near the surfaces of the cylinders. The following paragraphs describe our observations.

The phase lag between two hot wires located by the inner sides of the cylinders, at stations 2 and 3 of figure 1(*b*), was measured in the natural and in the excited flow. Both cases showed zero phase lag and high coherence at the higher shedding frequency ($S = 0.37$, natural and 0.26 , excited). Thus, vortex shedding from the inner separation points is in phase, as it would be in a two-dimensional jet (Foss & Korschelt 1983). No coherence was found at the lower frequency. This absence of coherence between the inner shear layers suggests that the lower frequency is associated with the outer separated layers. The lower frequency is also associated with larger vortices, which roll up farther downstream: Bearman & Wadcock (1973) and Williamson (1985) found that the low frequency became predominant far downstream in the flow.

The phase difference between the inner and outer separation points (stations 3 and 4, or 1 and 2) in the natural flow was 180° at the higher shedding frequency. This 180° phase angle is as in vortex shedding from a single cylinder. Again the lower shedding frequency showed no coherence suggesting that this frequency has little effect at the inner separation point.

Measurements made in the excited flow showed that the coherence between the inner and outer shear layers, which existed in natural flow, was destroyed by excitation. The inner shear layers remained correlated at the higher shedding frequency, with zero phase lag. Thus, when quasi-steady flopping is eliminated, the excitation also decouples the vortex shedding at the inner separation point from that at the outer separation point. It would appear that the higher-frequency shedding is no longer analogous to that of a single cylinder. Rather, the gap flow responds to excitation as would a two-dimensional jet.

The statistical picture of vortex shedding in the natural flow, which emerges from the above phase measurements and from the conditional spectra of figure 8, is similar to the instantaneous photographs taken by Williamson (1985) at low Reynolds number. Thus, the cylinder with the narrow wake sheds an antisymmetric vortex street, the flow through the gap carries a symmetric street, while the outer shear layer of the broader wake carries a vortex street having a longer wavelength.

Figure 22 shows smoke-wire visualizations in the natural and acoustically excited flows. In (*a*), the natural flow is showing a nearly to 3 to 1 ratio in vortex-shedding frequencies. One sees clearly that the lower shedding frequency is associated with roll-up well downstream of the cylinders. Although this is somewhat circumstantial, a smoke filament diverted toward the upper, higher-shedding-frequency shear layer is visible between the cylinders; the diversion of this filament toward the high-frequency side is in accord with our hot-wire data.

Figure 22(*b*) shows the flow with excitation at $fd/U_\infty = 1.45$. Immediately downstream of the cylinders small eddies, associated with the excited instability waves, are visible. Farther downstream a pattern of vortices seems to emerge. One sees that, on average, the excitation has made the wake nearly symmetric. Because the present study is focused on flopping in the flow near to the cylinder, we have not examined the downstream wake quantitatively.

6. Concluding remarks

It has been our purpose here to catalogue our observations of the flow between two parallel circular cylinders in the flopping regime. The splitter plate and excitation studies were undertaken with the objective of providing clues to the mechanics responsible for flopping; at present we shall not speculate on the detailed mechanism that is responsible for the asymmetry and flip-flopping.

Although the view that the flopping might be described as the behaviour of a dynamical system with two quasi-stable states does not do justice to the complexity of the fluid dynamics, such a viewpoint might ultimately lead to a deeper understanding of the flow. The flopping could be imagined to arise from a loss of stability by the symmetric mean flow as the cylinders are brought into proximity. Thus, figures 2 and 3 describe a sort of inverted bifurcation at $s/d = 1$ (in the sense that the solid curve breaks into two branches there). A simple dynamical system with two quasi-stable states, such as that described in Guckenheimer & Holmes (1983, p. 84), might describe the chaotic behaviour that ensures: the figures on that page bear some similarity to our figure 4. Reference to this example from Guckenheimer & Holmes makes the point that the flip-flopping can arise in a deterministic manner. Indeed, the flip-flopping seems insensitive to ambient noise: the large perturbations due to wake turbulence and vortex shedding do not seem to trigger the flip-flopping.

A fluid-dynamic analysis of the loss of stability would relate it to one wake closing more rapidly than the other. For example, the low pressure created thereby behind one cylinder might (almost) stably divert the gap flow. At larger cylinder spacing ($s/d > 1$) the base pressure difference associated with the diversion of the gap flow might be insufficient to maintain asymmetry. While it is not clear why flopping occurs, our hope is that the present investigation will contribute to its understanding.

REFERENCES

- BEARMAN, P. W. & WADCOCK, A. J. 1973 *J. Fluid Mech.* **61**, 499.
 BLOOR, M. S. 1964 *J. Fluid Mech.* **19**, 290.
 FOSS, J. F. & KORSCHULT, D. 1983 *J. Fluid Mech.* **132**, 79.
 GUCKENHEIMER, J. & HOLMES, P. 1983 *Nonlinear Oscillations, Dynamical Systems and Bifurcations of Vector Fields*. Springer.
 HAYASHI, M., SAKURAI, A. & OHYA, Y. 1983 *Trans. Japan Soc. Aero. Space Sci.* **26**, 22.
 MOOD, A. M., GRAYBILL, F. A. & BOES, D. C. 1974 *Introduction to the Theory of Statistics*. McGraw-Hill.
 WILLIAMSON, C. H. K. 1985 *J. Fluid Mech.* **159**, 1.
 WYGNANSKI, I. & PETERSEN, R. A. 1985 *AIAA paper* 85-0539.
 ZDRAVKOVICH, M. M. 1977 *Trans. ASMEI: J. Fluids Eng* **99**, 618.